Direct cooling from the regenerators of Gifford-McMahon cryocoolers, with comparison to pulse tube refrigerators

Ryan Snodgrass and Joel Ullom

National Institute of Standards and Technology, Boulder, CO 80305, USA

Department of Physics, University of Colorado Boulder, Boulder, CO 80309, USA

Abstract

The second-stage regenerators of pulse tube refrigerators (PTRs) are routinely used to intercept heat loads without disturbing cooling at their base temperatures, often near 4 K. Gifford-McMahon cryocoolers (GMCs) have not yet demonstrated a similar capability to provide regenerator cooling, possibly because of the thermal resistance between their regenerator shell and core. Here we show that GMCs do have capacity to provide regenerator cooling when heat loads are applied directly on the outer regenerator shell, although to a lesser extent compared to PTRs of similar cooling capacity. For example, we intercepted a 900 mW heat load at 21.6 K using the second-stage regenerator of a GMC while only giving up 10 mW of cooling at 3 K (out of 270 mW). This performance may possibly be improved by optimizing heat exchange between heat source and regenerator shell. We provide detailed temperature profile measurements from both a GMC and a PTR while applying heat to the regenerators, showing distinct behavior between the two. We also show that for GMCs, the optimal location of heat injection should be farther from the cold end than for PTRs. Although the physical source of regenerator cooling is less clear for GMCs than it is for PTRs, a useful amount of cooling is available and warrants further study.

Keywords: Regenerator cooling, intermediate cooling, pulse tube refrigerator, Gifford-McMahon cryocooler, thermoacoustics

1. Introduction

It is well known that the second-stage regenerators of low-frequency pulse tube refrigerators (PTRs) can intercept heat loads without significantly degrading the cooling available at the cold end temperature, usually near 3 K or 4 K

Email address: ryan.snodgrass@nist.gov

[1–6]. This capability has been used for many years in commercial systems; for example, many ^{3}He–^{4}He dilution refrigerators use regenerator cooling to absorb a significant portion of the circulating ^{3}He enthalpy.

As far as we aware, it has not been extensively studied if Gifford-McMahon cryocoolers (GMCs) can support similar regenerator cooling. In a GMC, there is a helium-filled gap between the outer regenerator shell and the surface of the displacing regenerator (in a PTR, the regenerator is stationary and the outer shell is in direct contact with the regenerator matrix). The gap between outer regenerator shell and displacer in GMCs inhibits heat transfer to the core from any heat exchanger mounted to the outer surface; however, the severity of this inhibition is unknown. In this study, we instrumented the second-stage regenerator of a GMC with an array of thermometers and heat exchangers to determine if any regenerator cooling is available despite the helium gap.

We found that GMC regenerators do have the capability to provide cooling without significantly affecting performance at the cold heat exchanger; however, the quality of that cooling is inferior to that available from a PTR. While a PTR regenerator can provide several watts of cooling at a temperature relatively close to the cold end temperature T_c [5–7], these first results suggest that a comparable GMC regenerator can only provide watt-scale cooling at locations far from the cold end, where the temperature of the regenerator is closer to the warm end temperature T_w. Heat injected closer to the cold end of the GMC resulted in a large degradation to the amount of cooling available at the cold heat exchanger.

Temperature profile measurements—combined with our interpretation of power flows in PTR regenerators [5, 6]—do not provide a clear understanding of how the GMC regenerator provides its cooling. As we show in the following, the response of the regenerator's temperature profile to heat is very different between the PTR and GMC.

2. Methods

All GMC measurements come from a Sumitomo RDK-415D, which has a nominal cooling power of 1.5 W at 4.2 K.[1] This cryocooler was operated with its cold end facing upwards. A total of 12 silicon diode thermometers (calibrated to an accuracy of $\pm$ 25 mK at temperatures < 25 K and to $\pm$ 75 mK at higher temperatures) were fastened to the second-stage regenerator using an array of copper clamps that fit snugly around the regenerator shell (Fig. 1). A thin layer of Apiezon N grease was applied between these clamps and the regenerator shell. The clamps and thermometers were arranged to measure the regenerator's temperature at seven x/L locations between its cold and warm end, where

[1]Certain commercial products are identified to specify the experimental study adequately. This does not imply endorsement by NIST or that the products are the best available for the purpose.

x is the axial distance along the regenerator measured from the warm heat exchanger, and L is the regenerator length.

Each clamp pair is composed of two semicircular, copper clamps (Fig. 1 isometric view) fastened together using stainless steel screws. The two copper clamp halves do not directly touch one another and are thermally linked only by the stainless steel screws and the regenerator shell. The temperature of both clamp halves was measured at five of the seven x/L locations. The temperature of the warm and cold heat exchangers was also measured using two additional silicon diodes. All temperature measurements reported here were made at steady state; our algorithm considered the cryocooler in steady state if all temperature measurements changed by less than 32 mK over a one minute time span.

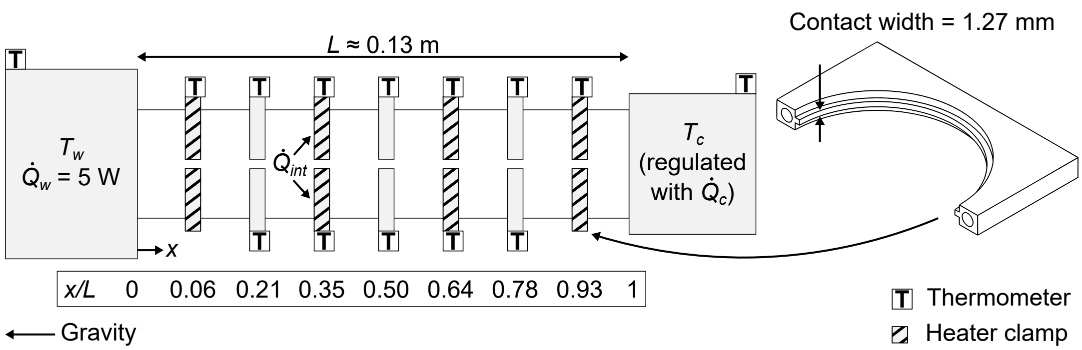

Figure 1: Gifford-McMahon cryocooler second-stage regenerator (of length L) and heat exchangers. At the warm heat exchanger ($x/L = 0$), a constant heat of 5 W was applied. At the cold heat exchanger ($x/L = 1$), the temperature was regulated to T_c (3 K unless otherwise stated). Isometric view shows one half of a copper clamp pair; a pair was fixed at each x/L to measure temperature or inject heat.

Four of the seven clamp pairs also have resistors epoxied (Stycast 2850FT) into cutouts so that heat may be applied to the regenerator along its length. These resistors are epoxied into both clamp halves, and heat is applied in an azimuthally-uniform manner. We call this heat $\dot{Q}_{int}$ (intermediate heat) because it is applied at intermediate temperatures between the warm T_w and cold T_c ends of the regenerator. Up to 3.375 W can be applied to each clamp pair—accomplished using a 90 V, pulse-width modulated signal.

We attempted to fix T_w using a commercial temperature controller, but were unsuccessful because of sporadic changes in temperature that were not correlated to the input heat. Instead, we applied a constant 5 W heat load at the warm end ($\dot{Q}_w = 5$ W) for all experiments. The cold end was regulated to its target temperature T_c (usually 3 K) using heat $\dot{Q}_c$ from the temperature controller.

The copper clamps used for thermometry and heat injection made contact with the regenerator shell over a circumferential band just 1.27 mm thick. This thickness was chosen to minimize the length of the regenerator that was thermally shorted by the highly conductive copper, but may also limit the heat transfer between clamp and stainless steel shell.

3. Results

3.1. Response to intermediate heat applied at different regenerator locations

The cold heat exchanger was regulated to 3 K while up to 3.3 W of heat was applied at four different locations along the regenerator, at $x/L = 0.06$, 0.35, 0.64, and 0.93. For the two heat injection locations closer to the warm end, the loss in cooling power at 3 K was minimal. For example, $\dot{Q}_c$ dropped from 270 mW to 240 mW when $\dot{Q}_{int} = 3.3$ W was applied at $x/L = 0.35$ (Fig. 2a). At heat injection locations closer to the cold end, $\dot{Q}_c$ dropped more significantly with increasing $\dot{Q}_{int}$; for example, with 0.9 W of heat applied at $x/L = 0.93$, almost all of the cooling power at 3 K was exhausted.

The temperature of intermediate heat injection is shown by two different metrics in the next subplots. Figure 2b plots T_{heat} versus $\dot{Q}_{int}$, where T_{heat} is the average (considering both clamp halves) temperature measured on the active heater. This is the true temperature of heat injection, but is influenced by the design of our intermediate heat exchangers. Because the copper clamps are not brazed to the regenerator shell and only make contact with the regenerator over a 1.27 mm width (Fig. 1), their heat transfer to the shell is limited. Using cubic spline fits of the entire temperature profile between $x/L = 0$ and 1 (shown later in the manuscript), we also calculated the temperature of the regenerator shell T_{reg} at the x/L where heat was injected using all temperature measurements except those at the injection location. That result is plotted in Fig. 2c. If heat exchange to the regenerator shell was improved, a heat injection temperature between T_{heat} and T_{reg} (which is significantly lower than T_{heat} at large $\dot{Q}_{int}$) should be achieved; however, the thermal resistance between outer stainless steel shell and regenerator core might still dominate the total thermal resistance, so it is unknown how large of an improvement is possible. To be conservative, we use T_{heat} in the remainder of the manuscript.

Returning to Fig. 2b, it can be seen that a useful amount of cooling can be extracted from the GMC regenerator. Consider the $x/L = 0.35$ curve: T_{heat} is below the temperature of the warm heat exchanger T_w for $\dot{Q}_{int} \leq 2.1$ W, so heat loads up to 2.1 W can be cooled to an intermediate temperature at this particular location. This extra source of cooling is achieved with minimal effect to the warm and cold heat exchangers. For example, when 900 mW of heat is injected at 21.6 K, T_w only rises from 32.3 K to 32.8 K and $\dot{Q}_c$ only decreases from 270 mW to 260 mW.

Some insight into how intermediate heat affects the total power flow [5, 6, 8] through the regenerator may be gained by analyzing the temperatures near the warm and cold ends. The temperature at $x/L = 0.93$ is plotted in Fig. 2d, and shows that this temperature rises more significantly when heat is applied nearer the cold end. Two components of total power flow are directly proportional

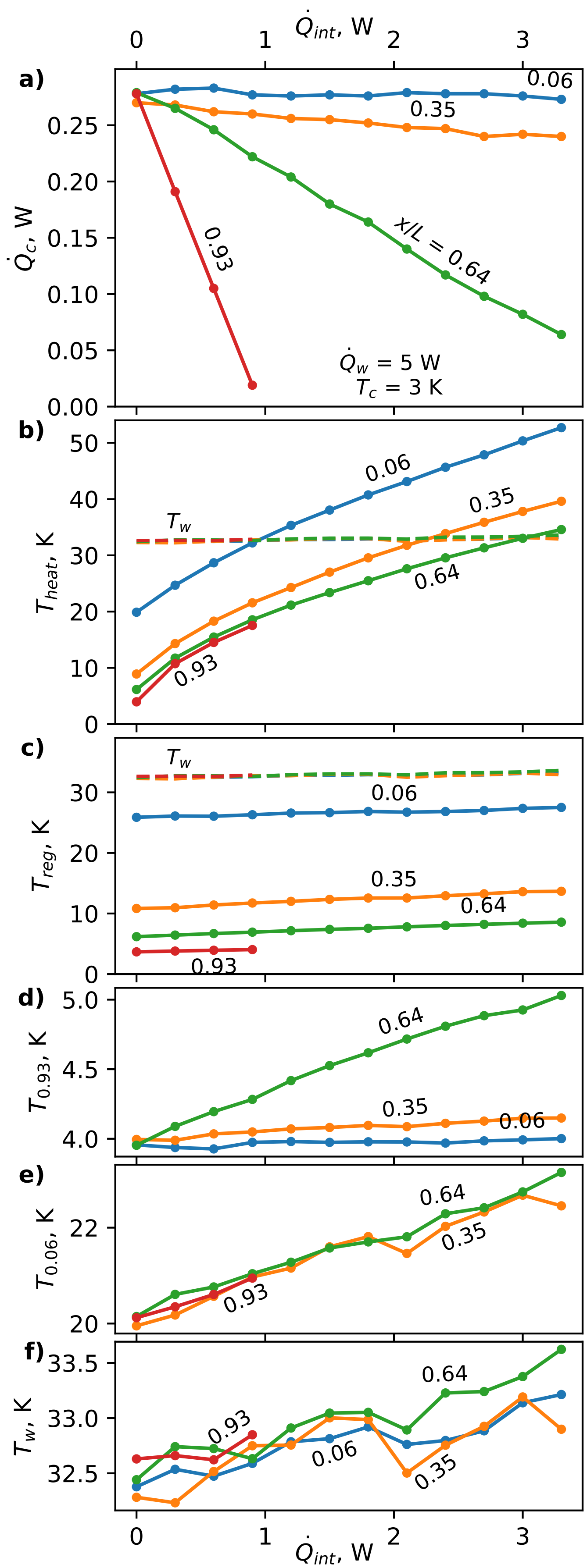

Figure 2: (Caption on following page.)

Figure 2: Response of a Gifford-McMahon cryocooler with intermediate heat $\dot{Q}_{int}$ applied at four different x/L locations. The cold end was regulated to 3 K while a constant 5 W was applied to the warm end. a) Cooling power at 3 K. b) The temperature of the intermediate heater, as measured with thermometry placed directly on it. For $x/L = 0.35$ and 0.64, this value is the average from the thermometers on both clamp halves. For comparison, the dashed lines (which are barely distinguishable) plot the warm end temperatures as $\dot{Q}_{int}$ varies. c) The temperature of the regenerator at the location of the heater, calculated from a cubic spline fit of the temperature profile that included all temperature measurements except those at the location of the heater. d) The temperature measured at $x/L = 0.93$ (data for heat injected at $x/L = 0.93$ intentionally excluded). e) The temperature measured at $x/L = 0.06$ (data for heat injected at $x/L = 0.06$ intentionally excluded). f) The temperature of the warm heat exchanger.

to the magnitude of the temperature gradient. One of those components is conduction, and the other is proportional to $|U_1|^2$, where U_1 is the complex, oscillating volume flow rate of the fluid. Higher temperature gradient leads to more power flowing down the regenerator towards the cold heat exchanger, which directly subtracts from $\dot{Q}_c$. Therefore, an increase in the magnitude of the temperature gradient at the cold end may explain the increased sensitivity of $\dot{Q}_c$ to $\dot{Q}_{int}$ for injection locations nearer $x/L = 1$.

While the temperature at $x/L = 0.93$ is sensitive to the heat injection location, the temperatures at $x/L = 0.06$ (Fig. 2e) and $x/L = 0$ (Fig. 2f) are not. This may suggest that when heat is applied to the regenerator of a GMC, much of it flows towards the cold end (which is in contrast to the behavior in PTRs [5, 6]). The response of the temperature profile to intermediate heat will be discussed further in Section 3.3, where we compare regenerator cooling using Gifford-McMahon cryocoolers and pulse tube refrigerators.

3.2. *Absorbing ^{4}He enthalpy using the GMC regenerator*

The utility of the regenerator cooling presented in Section 3.1 will depend upon the use-case. In this subsection, we consider a common application of GMCs: ^{4}He liquefaction. Although we did not condense ^{4}He experimentally, we predict the performance of ^{4}He enthalpy absorption by inputting the data from Fig. 2 into a simple model.

Consider a ^{4}He stream with molar flow rate $\dot{N}_4$ that must be cooled to T_c using the GMC. We ignore any loads on the first stage and start our analysis with ^{4}He leaving the first-stage heat exchanger at a temperature of $T_w = 32.3$ K. The fluid then passes through a heat exchanger on the second-stage regenerator, exiting with a temperature T_{heat}. The amount of enthalpy absorbed by the regenerator is

$$\dot{Q}_{int} = \dot{N}_4[h(T_w) - h(T_{heat})], \tag{1}$$

where h is the molar enthalpy of ^{4}He at 1 atm. After the regenerator heat exchanger, the fluid is routed to the cold end at temperature $T_c = 3$ K, depositing the remainder of its enthalpy on the second-stage heat exchanger:

$$\dot{Q}_2 = \dot{N}_4[h(T_{heat}) - h(T_c)]. \tag{2}$$

In this simplified analysis, we do not account for finite heat exchange: the temperature of the fluid is assumed equal to that of each heat exchanger. The temperatures at the warm and cold ends that were chosen for this analysis were restricted by the data from Fig. 2; in practice, more helium could be condensed for 4.2 K $> T_c >$ 3 K.

We applied spline fits to the data from Fig. 2b and iteratively input (T_{heat}, $\dot{Q}_{int}$) pairs into Eq. (1) until satisfied. The resultant regenerator heat exchanger temperatures and heat loads on the regenerator are shown in Fig. 3a and Fig. 3b (respectively) as a function of ^{4}He flow rate. As expected, T_{heat} is lower and $\dot{Q}_{int}$ higher for heat injection locations closer to the cold end. However, since the heater temperatures differ from one another by only about 5 K for $x/L =$ 0.35, 0.64, and 0.93, the amount of enthalpy absorbed by the regenerator only differs by about 40 mW or less. Data from $x/L = 0.06$ is not shown because the temperature there is at least 10 K higher than the other locations (Fig. 2b), so significantly less enthalpy can be absorbed by the regenerator.

Figure 3c plots the remaining cooling power $\dot{Q}_c$ available at 3 K as the helium flow rate increases. Cooling power at the cold end is impacted by two sources. The first heat load is the deposition of the ^{4}He enthalpy at the cold end (Eq. (2)), which includes the latent heat of condensation. The second is the effective load on the cold end that results from applying intermediate heat to the regenerator. This latter quantity ($\dot{Q}_{drop}$) was calculated using the data from Fig. 2a and is plotted in Fig. 3d. Recall that $\dot{Q}_{drop}$ is more significant when heat loads are placed closer to $x/L = 1$.

For comparison, Fig. 3c also shows $\dot{Q}_c$ as a function of $\dot{N}_4$ without regenerator cooling: in this case, about 0.38 mmol/s of ^{4}He can be cooled to 3 K before exhausting the cold end's cooling power. With regenerator cooling at $x/L = 0.35$, 0.64, and 0.93, about twice as much helium can be condensed: 0.81 mmol/s, 0.86 mmol/s, and 0.69 mmol/s, respectively. Roughly speaking, the optimal heat sink location is where the regenerator has its lowest temperature (so a large amount of enthalpy can be absorbed by the regenerator) while also being far enough away from $x/L = 1$ to not significantly increase the magnitude of the temperature gradient at the cold end. This is illustrated by the $x/L =$ 0.93 data, where the maximum $\dot{N}_4$ is lower than for $x/L = 0.35$ and 0.64 because of the larger contribution from $\dot{Q}_{drop}$. We have studied optimal intermediate heat exchanger locations in more detail using PTRs [7].

The calculations for ^{4}He absorption (Eqs. (1) and (2)) used the conservative measurement for heat injection temperature (T_{heat}). If heat transfer from the intermediate heat exchanger to the regenerator core was improved, temperatures between T_{heat} and T_{reg} (see Section 3.1) should be achievable. Performing the same calculations assuming a heat injection temperature of $(T_{heat}+T_{reg})/2$, the maximum helium flow rate before $\dot{Q}_c$ is exhausted improves from 0.86 mmol/s to 1.01 mmol/s ($x/L = 0.64$). We do not present the full results with this less-conservative estimate of the injection temperature because we are uncertain by

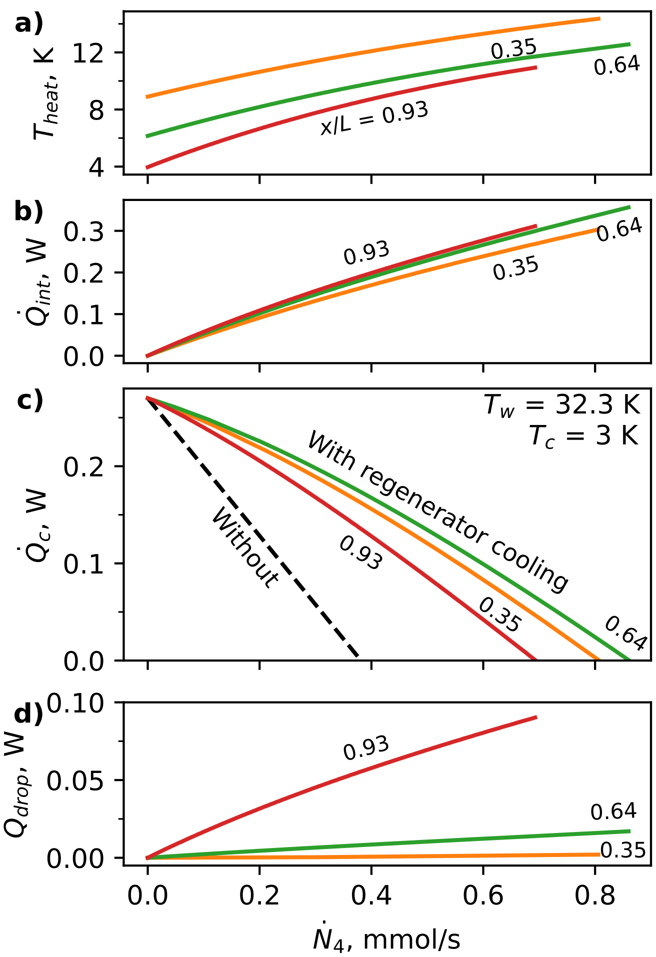

Figure 3: Model of ^{4}He enthalpy absorption using a heat exchanger placed on the GMC regenerator. a) The temperature of the regenerator heat exchanger and b) the heat absorbed by the regenerator for flow rates $\dot{N}_4$ up to about 1 mmol/s, considering heat exchange locations of $x/L = 0.35$, 0.64, or 0.93. These parameters were calculated using Eq. (1) and the experimental data from Fig. 2b. Each line ends when the cooling capacity at 3 K is exhausted, as plotted in c). The model was simplified by assuming the warm end temperature is insensitive to $\dot{N}_4$ and fixed at 32.3 K. The dashed line in subplot c shows how $\dot{Q}_c$ would decrease without regenerator cooling, i.e. if all the enthalpy between T_w and T_c was absorbed at the cold end. For the solid lines, the decrease in $\dot{Q}_c$ comes from two sources. First, the ^{4}He enthalpy to absorb between T_{heat} and T_c; second, the impact of the regenerator heat load on the cold end, which is plotted in d) and comes from Fig. 2a.

how much the heat transfer to the regenerator core can be improved.

3.3. Comparison to pulse tube refrigerator

We have extensively characterized a Cryomech PT407 pulse tube refrigerator (PTR) and its capability to absorb intermediate heat loads with its second-stage regenerator [5–7, 9]. This refrigerator has a nominal cooling capacity of 0.7 W at 4.2 K. We instrumented the PT407 in a very similar manner as the RDK-415D Gifford-McMahon cryocooler, except we mounted a greater number of copper clamps to the regenerator so that between 9 and 11 temperature measurements could be made between the warm and cold ends (the spatial resolution of these measurements was about 1.5 cm). The design of the copper clamps was identical to that shown in Fig. 1 except that the diameter of the central cutout was modified to match the PT407 regenerator. Please see our other publications for more information on the intermediate cooling available from PTR regenerators.

3.3.1. Temperature profile and cold-end cooling power

When a moderate amount of heat is applied to a PTR regenerator operating in the real-fluid regime, the total power flow [5, 6] upstream of heat injection (towards the warm end) lessens by the amount of heat applied, while the total power flow downstream of heat injection (towards the cold end) stays nearly fixed. Because the total power flowing into the cold heat exchanger is unchanged, the cooling power at T_c is not disturbed by the intermediate heat load[2].

Changes to total power flow in the PTR are evident by the shape of the temperature profiles shown in Fig. 4a. Near the warm end, some fraction of total power is carried by power terms that are directly proportional to the negative of the temperature gradient. As $\dot{Q}_{int}$ is increased, the magnitude of the temperature gradient at the warm end and the total power flux there both decrease. Behavior at the cold end is different: the temperature profile there does not change when intermediate heat is applied, so total power flow stays constant[3]. Figure 4b confirms this behavior: even with 2.4 W of heat applied to the regenerator, cooling power at 3 K only drops from 249 mW to 247 mW.

In Fig. 4, we compare the PTR to the GMC for a similar heat injection location ($x/L = 0.64$ or 0.65). The GMC shows much different behavior compared to the PTR. Figure 4a shows that when heat is applied, all portions of the temperature profile rise (besides the regulated cold end), and Fig. 4b shows that the drop in cooling power is significant (but still much less than $\dot{Q}_{int}$). As discussed in Section 3.1, the impact on $\dot{Q}_c$ is heavily dependent upon the heat injection location.

The temperature profile and cooling power measurements suggest that intermediate heat loads should be placed farther from the cold end in GMCs than

[2]The total power flowing out of the cold heat exchanger (into the buffer tube) is also roughly fixed and equal to the acoustic power. A First Law analysis at the cold heat exchanger then gives fixed cooling power. See [5, 6] for more details.

[3]Assuming no changes to the streaming mass flows or to the acoustic power.

in PTRs. For the PTR, Fig. 4a shows that the temperature profile is only affected about $0.15x/L$ downstream of heat injection, so that $\dot{Q}_c$ is not changed when heat is applied at $x/L = 0.65$. The GMC, however, shows significant temperature profile change all the way to $x/L = 0.93$ for a similar heat injection location, so that total power flow into the cold heat exchanger may be increased by power terms proportional to the negative of the temperature gradient.

3.3.2. Thermal connection to regenerator core

Figure 4c plots the difference between the temperature of the heater T_{heat} and the temperature of the regenerator shell at the location of the heater T_{reg}. This temperature difference is roughly twice as large for the GMC as for the PTR, confirming that it is more difficult to transfer heat to the core of a GMC regenerator.

The increase in $T_{heat} - T_{reg}$ for the GMC should be unrelated to our experimental methods, as the intermediate heat exchangers were of the same design for both cryocoolers (same material and contact width) and were fixed to the regenerator using the same strategy: firmly bolting together the two clamp halves around the stainless steel shell. The outer diameter of the GMC's regenerator is about 45% larger than the PTR's; even though the GMC's clamps had 45% more area to transfer heat over, Fig. 4c shows the clamps rising in temperature much more significantly for the same intermediate heat load when compared to the PTR.

3.3.3. Temperature asymmetry

The following two subsections compare behavior of the temperature profile in PTRs and GMCs when no heat is applied to the regenerator. First we consider temperature asymmetries, and second we consider the overall shape of the temperature profile. These observations are included here because they may assist in identifying power flows in the regenerator; these power flows are central to understanding cryocooler performance.

We recently reported azimuthal temperature differences in pulse tube refrigerator regenerators operating in the real-fluid regime [9]. At certain combinations of T_w and T_c, one half of the regenerator may be significantly colder than the opposing half (at the same x/L) over a portion of its length, so that the temperature profile cannot be described using only the axial coordinate x.

To investigate whether similar temperature asymmetries may exist in GMCs, the temperature on both halves of the GMC regenerator shell was measured at $x/L = 0.21$, 0.35, 0.5, 0.64, and 0.78. Experiments were performed with T_c controlled between 3 K and 22 K (including 4.5 K, 5.5 K, 7 K, 9 K, and 16 K), while $\dot{Q}_w$ was fixed at 5 W (resulting in T_w between 32 K and 40 K). Even across this large range of end conditions, no significant azimuthal temperature variation was observed. The maximum temperature asymmetry measured at any single x/L was 0.4 K, compared to temperature differences of up to 15 K measured in the PTR studied in our previous work [9]. Perhaps it is possible that azimuthal components of flow in the gap between shell and displacer in a GMC can suppress temperature asymmetries.

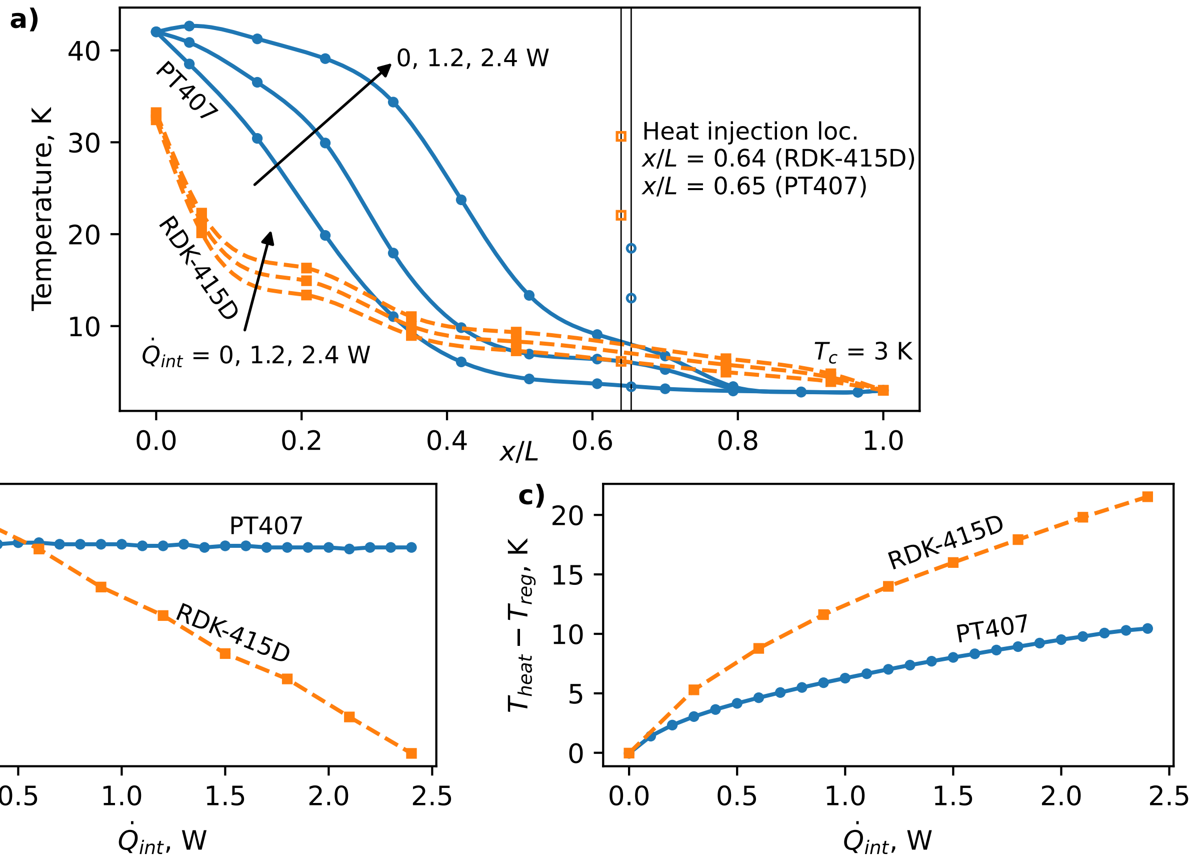

Figure 4: Intermediate heat applied at the same regenerator location for both PTR and GMC. a) Temperature profile response when heat was applied at $x/L = 0.65$ (PTR, solid blue lines) or $x/L = 0.64$ (GMC, dashed orange lines). Heat injection locations are shown by the vertical lines. Intermediate heats of 0 W, 1.2 W, and 2.4 W were applied while the cold end was regulated to 3 K. For the PTR experiments, the warm end was regulated to 42 K, while in the GMC experiments a constant 5 W was applied to the warm end. The markers shown at the heat injection location give the temperatures measured on the heater (T_{heat}), which were not included in the cubic spline fits. Subplots b and c are from the same experiments as subplot a. b) Cooling at 3 K while intermediate heat was incremented. c) The temperature difference between the heater T_{heat} and the regenerator at the location of heat injection T_{reg}, where T_{reg} was calculated using the cubic spline fits shown in subplot a.

3.3.4. Temperature profile inversion

The following considers the overall shape of the temperature profile, and builds off of total power flow analysis contained in our previous works [5, 6]. For the most-complete understanding of this section, we recommend reviewing those sources.

Total power flow [5, 6, 8] is constant at all axial positions of a regenerator operating in steady-state when no external heat is applied to it[4]. The temperature profile between T_w and T_c takes whichever form necessary to conserve total power flow as fluid and material properties change with temperature. At the warm end of the regenerator, helium is an ideal gas and the heat capacity of the regenerator material is large compared to that of the fluid, so power flow terms associated with temperature (as opposed to temperature gradient) are relatively small. At the cold end of a 3 K or 4 K regenerator, the power flow terms associated with real-fluid effects are very large [5, 6]. This difference in power flow terms associated with temperature results in a flat temperature profile at the cold end and a steep temperature profile at the warm end.

If T_c is raised above 4 K enough such that the power terms related to real-fluid effects become small, it is possible for the temperature profile to invert from its normal state. In an inverted profile, the temperature gradient is nearly zero at the warm end but large at the cold end. Because power flow terms associated with temperature are larger at T_w than at T_c, a significant temperature gradient is required at the cold end to conserve total power flow. This radical change in the shape of the temperature profile was predicted by de Waele [10].

Profile inversion in a PTR can be seen in Fig. 5. At T_c less than about 7 K, the profile is normal and nearly flat at the cold end. At T_c above about 7 K, the profile inverts and is nearly flat at the warm end. Figure 5 shows that the same behavior does not occur for the GMC used in this study: even with T_c raised to 16 K, no profile inversion takes place.

The absence of temperature profile inversion may be related to regenerator materials. Although we are unaware of which materials are inside this GMC's regenerator, such behavior should be possible if the matrix material at the cold end has relatively large heat capacity near 4 K but much lower heat capacity at higher temperatures (there are such materials that are commonly used in the construction of regenerators). Near 4 K, real-fluid power terms are large and cause the profile to be flat at the cold end. As T_c is increased, real-fluid power terms begin to decrease; however, for such a material there is a simultaneously increase in the finite-heat-capacity power term. The real-fluid power term and the finite-heat-capacity power term may add together such that the temperature-associated power terms are always larger at T_c than at T_w.

[4]Ignoring possible effects from temperature asymmetries.

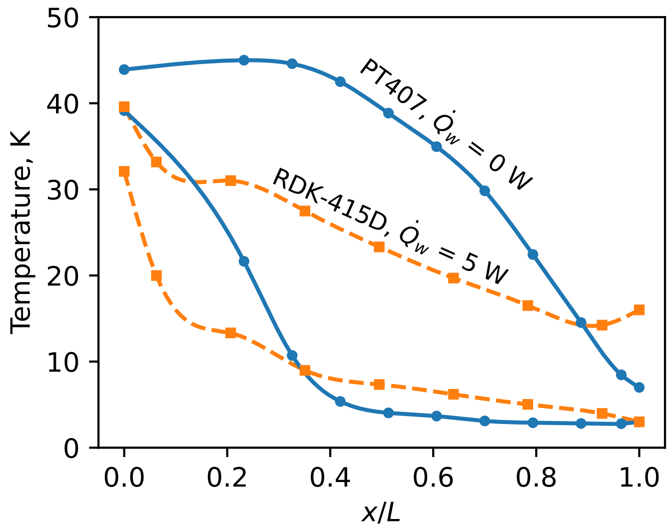

Figure 5: Temperature profile inversion. The pulse tube refrigerator's temperature profile (solid blue lines) transitions from flat at the cold end to flat at the warm end when T_c is regulated to temperatures higher than about 7 K (this transition temperature is also dependent upon T_w). The GMC (dashed orange lines) does not display the same transition in profile shape, even when the cold end is regulated to 16 K. The cubic spline fits shown here were calculated using the mean temperatures (temperature was measured on opposing halves of both regenerators). For both PTR profiles, no heat was applied at the warm end. For both GMC profiles, 5 W was applied at the warm end.

4. Discussion

In pulse tube refrigerators, significant amounts of intermediate heat may be applied to the regenerator operating in the real-fluid regime without affecting the cooling available at the cold heat exchanger. Analysis of the temperature profile [5, 6] suggests that this is possible because only power flow upstream of heat injection (towards the warm end) is affected by the injected heat, while power flow at the cold end is unaffected.

As shown here, a useful amount of cooling may also be extracted from the second-stage regenerators of Gifford-McMahon cryocoolers; however, compared to a PTR, changes to total power flow are less clear, and obscure which mechanisms enable regenerator cooling. When intermediate heat is applied to a GMC, the temperature increases nearly everywhere in the regenerator. This observation may suggest that the movement of the displacer and the surrounding helium cause the injected heat to be absorbed over much of the regenerator's length instead of at a discrete location. In GMCs, the temperature of the regenerator very near the cold heat exchanger increases more significantly (compared to PTRs) when heat is applied closer to it, so intermediate cooling is only without consequence when the regenerator heat exchanger is placed far from the cold end. For the particular cryocooler studied here, $x/L = 0.35$ seemed to give a good compromise between intermediate heat exchange temperature and the drop in cooling power at the cold end. Good locations to inject heat may vary for GMCs with significantly different temperature profiles.

A further compromise for GMCs is that the heat transfer between regenerator heat exchanger and regenerator core is poor compared to PTRs. For heat to reach the core, it must pass through two solid surfaces (the outer shell and the wall of the displacer, both of which must be constructed of low thermal conductivity materials) and a helium-filled gap. It is possible that the gap between the outer shell and displacer dominates the total thermal resistance between regenerator heat exchanger and core; however, we are unable to make reasonable estimates without information on wall thicknesses, the size of the gap, and the flow characteristics in the gap. Nonetheless, our methodology represents the worst-case scenario of what should be achievable by the average user, as our intermediate heat exchangers were not brazed to the regenerator shell, and made contact with the shell over a width of about 1 mm. It is unknown whether brazing to the outer shell is feasible without impeding the axial motion of the regenerator.

We also studied how the regenerator of a GMC may be used to support ^{4}He liquefaction and cooling to 3 K. We showed that more than double the ^{4}He flow rate can be cooled and condensed when a regenerator heat exchanger is used versus when it is not. More work is required to determine if regenerator cooling provides as much benefit at ^{4}He exit temperatures between 3 K and 4.2 K, where higher flow rates are possible and the heat load on the regenerator would be higher.

Given the ubiquity of GMCs and the limited knowledge of regenerator cooling using them, we recommend further study in this area.

5. References

References

[1] K. Uhlig, 3He/4He dilution refrigerator with pulse-tube refrigerator precooling, Cryogenics 42 (2) (2002) 73–77. doi:10.1016/S0011-2275(02)00002-4.

[2] A. Ravex, T. Trollier, J. Tanchon, T. Prouvé, Free Third-Stage Cooling for Two-Stage 4 K Pulse Tube Cryocooler, in: Cryocoolers 14, 2007, pp. 157–161.

[3] T. Prouvé, H. Godfrin, C. Gianèse, S. Triqueneaux, A. Ravex, Experimental results on the free cooling power available on 4K pulse tube coolers, Journal of Physics: Conference Series 150 (1) (2009) 012038. doi:10.1088/1742-6596/150/1/012038.

[4] C. Wang, Extracting Cooling from the Pulse Tube and Regenerator in a 4 K Pulse Tube Cryocooler, in: Cryocoolers 15, 2009, pp. 177–184.

[5] R. Snodgrass, V. Kotsubo, J. Ullom, S. Backhaus, Leveraging Real Fluid Effects as a Tool for Power Flow Measurements in 4 K Cryocooler Regenerators, Cryocoolers 21 (2021) 315–324.

[6] R. Snodgrass, G. Swift, J. Ullom, S. Backhaus, Intermediate cooling from pulse tube refrigerator regenerators operating in the real-fluid regime (In preparation).

[7] R. Snodgrass, J. Ullom, S. Backhaus, Optimal absorption of distributed and conductive heat loads with cryocooler regenerators, Cryogenic Engineering Conference 2021 (Accepted).

[8] G. W. Swift, Thermoacoustics: A Unifying Perspective for Some Engines and Refrigerators, 2nd Edition, Springer International Publishing, 2017. doi:10.1007/978-3-319-66933-5.

[9] R. Snodgrass, V. Kotsubo, J. Ullom, S. Backhaus, A Temperature Instability in 4 K Cryocooler Regenerators Caused by Real Fluid Properties, Cryocoolers 21 (2021) 305–313.

[10] A. T. A. M. de Waele, M. Y. Xu, Y. L. Ju, Nonideal-gas effect in regenerators, Cryogenics 39 (10) (1999) 847–851. doi:10.1016/S0011-2275(99)00102-2.

[11] J. D. Hunter, Matplotlib: A 2D Graphics Environment, Computing in Science Engineering 9 (3) (2007) 90–95. doi:10.1109/MCSE.2007.55.

[12] I. H. Bell, J. Wronski, S. Quoilin, V. Lemort, Pure and Pseudo-pure Fluid Thermophysical Property Evaluation and the Open-Source Thermophysical Property Library CoolProp, Industrial & Engineering Chemistry Research 53 (6) (2014) 2498–2508. doi:10.1021/ie4033999.

6. Acknowledgments

R.S. acknowledges support from a National Research Council Postdoctoral Fellowship, and from the Professional Research Experience Program (PREP) between the University of Colorado Boulder and NIST under award number 70NANB18H006. Figures were generated using Matplotlib [11] and fluid properties were obtained from CoolProp [12]. Manuscript is a contribution of NIST, and not subject to copyright. R.S. acknowledges guidance and support from Scott Backhaus and Vincent Kotsubo of NIST, and from Gregory Swift of Swift Science and Engineering.